THE JOURNAL OF PROSTHETIC DENTISTRY

RESEARCH AND EDUCATION

Dimensional precision of implant-supported frameworks fabricated by 3D printing

Anna Gabriella Camacho Presotto, DDS, MSc,[a] Valentim Adelino Ricardo Barão, DDS, MSc, PhD,[b] Cláudia Lopes Brilhante Bhering, DDS, MSc, PhD,[c] and Marcelo Ferraz Mesquita, DDS, MSc, PhD[d]

ABSTRACT

Statement of problem. Selective laser melting (SLM) is a promising additive technology for clinical practice, but data on dimensional precision assessed by marginal fit combined with stress and strain investigations of implant-supported fixed partial dentures (FPDs) are lacking.

Purpose. The purpose of this in vitro study was to verify whether the SLM additive manufacturing technology provides better dimensional precision for 3-unit FPD frameworks than subtractive manufacturing with soft metal block (SMB) milling and the standard casting technique.

Material and methods. Thirty 3-unit implant-supported FPDs with Co-Cr frameworks were made by the casting, SMB milling, and SLM methods (n=10). The marginal fit between the framework and the implant abutment was evaluated with photoelastic (PH) and strain gauge (SG) models. Stress and strain in the implant-supported system were measured by quantitative PH and SG analyses after prosthetic screw tightening. Data were subjected to the Kruskal-Wallis test, Mann-Whitney U test, and Spearman correlation test (α=.05).

Results. The framework manufacturing method affected the marginal fit (P<.001), stress, and strain values (P<.05). The SLM group showed the best mean ±standard deviation marginal fit (μm) (PH model: 8.4 ±3.2; SG model: 6.9 ±2.1) in comparison with SMB milling (PH model: 42.3 ±15.7; SG model: 41.3 ±15.3) and casting (PH model: 43.5 ±27.8; SG model: 41.3 ±24.6) (P<.05). SLM showed lower mean ±standard deviation stress and strain values (60.3 ±11.6 MPa; 91.4 ±11.1 μstrain) than casting (225.5 ±142.8 MPa; 226.95 ±55.4 μstrain) and SMB milling (218.6 ±101.7 MPa; 289.7 ±89.3 μstrain) (P<.05). A positive correlation was observed between fit and stress or strain for all groups (P<.05).

Conclusions. Three-unit FPD frameworks made using the SLM technology showed better dimensional precision than those obtained with the casting or SMB milling methods. (J Prosthet Dent 2019;122:38-45)

Fixed partial dentures (FPDs) in dentistry are usually manufactured by the lost-wax technique,[1-5] and casting procedures are an affordable option for patients who need base-metal restorations.[3,5] However, this conventional technique is complex and time-consuming.[6] To reduce the human factor and laboratory variables generated by the inconsistency of the volumetric and linear expansion of the materials used (impression materials, waxes, gypsum, casting investments),[7,8] computer-aided design and computer-aided manufacturing (CAD-CAM) systems have been introduced as a promising alternative to conventional casting techniques.[1,3,9-13]

CAD-CAM systems can be classified into subtractive manufacturing (SM) and additive manufacturing (3D printing). SM involves the fabrication of prostheses from block-shaped materials by using diamond rotary instruments.[1,3] One available SM technology is the milling of a soft metal block (SMB) with mechanical properties similar to those of a wax block. This feature provides advantages such as reduced stress on the milling machines and reduced milling time compared with hard metal blocks.[1] The FPDs made by the SMB milling technique were previously compared

Supported by the São Paulo Research Foundation (grant #2016/23490-1) and by the Coordenação de Aperfeiçoamento de Pessoal de Nível Superior, Brazil (CAPES) (Finance Code 001).
[a]Doctoral student, Department of Prosthodontics and Periodontology, Piracicaba Dental School, University of Campinas (Unicamp), Piracicaba, Brazil.
[b]Assistant Professor, Department of Prosthodontics and Periodontology, Piracicaba Dental School, University of Campinas (Unicamp), Piracicaba, Brazil.
[c]Assistant Professor, Department of Restorative Dentistry, School of Dentistry, Federal University of Minas Gerais (UFMG), Belo Horizonte, Brazil.
[d]Professor, Department of Prosthodontics and Periodontology, Piracicaba Dental School, University of Campinas (Unicamp), Piracicaba, Brazil.

Clinical Implications

Initial marginal fit, stress, and strain results indicate that the 3D printing selective laser melting technology is a promising method for fabricating implant-supported fixed partial dentures. Further investigations are warranted to fully clarify the long-term behavior of the technology for clinical practice.

with casted frameworks and showed similar marginal fit and stress; however, higher consistency was observed for SMB frameworks, a further advantage of the technique.[3,14,15] An important disadvantage of the method is material waste due to removing material from a block to fabricate the framework,[3] with up to 90% of the material being wasted.[11]

A recently introduced method for prosthesis fabrication without material waste, selective laser melting (SLM) additive manufacturing, has shown promising results for the fabrication of metal restorations.[10,12,16-20] The SLM additive technology is a 3D printing technology that allows for the direct impression of a metal prosthesis by sintering layers of metal powder, saving production time by improving efficiency.[16,18] The residual metal powder can be used for future fabrications, thus avoiding material waste.[1,21,22] Previous studies have evaluated FPDs fabricated by additive manufacturing and compared some biomechanical parameters with those of cast and/or subtractive frameworks.[10,12,20,23-29] However, only the fit and fracture properties of copings or FPDs were investigated, and marginal fit, stress, and strain investigations of implant-supported FPDs are lacking.

Therefore, the purpose of this in vitro study was to determine whether implant-supported FPDs with Co-Cr frameworks fabricated by SLM additive manufacturing provides better dimensional precision than those made by SMB SM and casting as evaluated by marginal fit, stress, and strain evaluations. The null hypothesis was that no difference would be found in the dimensional precision of FPD frameworks manufactured by using the 3 different technologies.

MATERIAL AND METHODS

A steel master model (30×20×15 mm) with 2 miniabutment analogs screwed onto 2 drillings placed 18 mm apart (center to center) was fabricated (Fig. 1). Cast miniabutment cylinders (Mini-abutment cylinder; SIN-Sistema de Implante) were screwed onto the analogs of the master model, and frameworks simulating an FPD of a mandibular first premolar (PM region) to a first molar (M region) were formed by using a low-shrinkage acrylic resin (GC Pattern Resin; GC America Inc). The

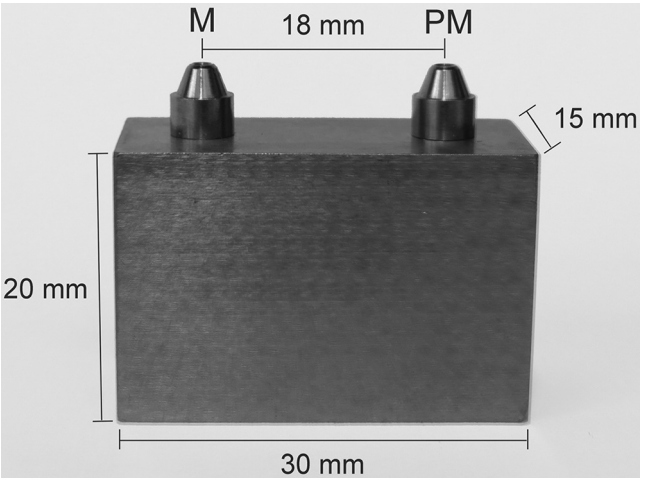

Figure 1. Master model with dimensions and regions (PM and M) designated. M, first molar; PM, first premolar.

framework was screwed onto the master model, and an impression (Flexitime Easy Putty Correct Flow; Kulzer GmbH) was made. This was duplicated to standardize the framework patterns (n=10). The frameworks were invested (Gilvest HS; BK Giulini) and cast in Co-Cr alloy (StarLoy C; DeguDent GmbH) (59.4% Co, 24.5% Cr, 10% W, 2% Nb, 2% V, 1% Si, 1% Mo, 1% Fe, and elastic modulus of 200 GPa) by the lost-wax casting technique (cast control group) (n=10). A furnace with a 35 °C/min increase in temperature was used, and the frameworks were heated for 30 minutes at 450 °C, 700 °C, and 850 °C. The frameworks were then slowly cooled for 40 minutes, abraded with Al_2O_3 particles (125 μm and pressure of 0.55 MPa) (Aluminum Oxide; Renfert Ltd), and finished and polished by using tungsten carbide burs at a low speed, except in the margin in contact with the abutment surface (Fig. 2A).

For the SMB milled frameworks (experimental group) (n=10), the master model and the assembled master model/waxed framework were scanned (Ceramill Map 300 Scanner; Amann Girrbach). The CAD files were imported into the respective software program (Ceramill map v2.7.05; Amann Girrbach), and the virtual model was acquired. The frameworks were milled in a milling machine (Ceramill Motion 2; Amann Girrbach) from Co-Cr blocks (Ceramill Sintron blocks; Amann Girrbach) (66% Co, 28% Cr, 5% Mo, <1% Si, <1% Fe, <1% Mn, <1% C, and elastic modulus of 200 GPa). After being milled, the frameworks were sintered at 1280 °C for 5 hours in the sintering box (Ceramill Sinter box; Amann Girrbach) of the sintering furnace (Ceramill Argotherm; Amann Girrbach). The specimens were finished with airborne-particle abrasion (125-μm Al_2O_3 particles; pressure of 0.55 MPa) (Fig. 2B).

For the SLM frameworks (experimental group) (n=10), the previously obtained CAD file was converted

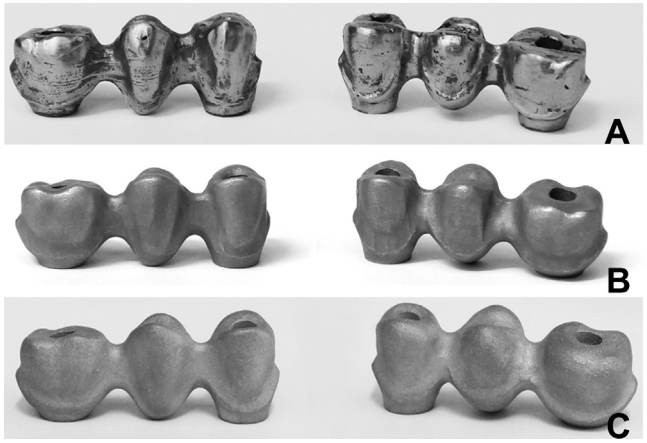

Figure 2. A, Cast frameworks. B, SMB frameworks. C, SLM frameworks. SLM, selective laser melting; SMB, soft metal block.

to standard tessellation language (STL) files and transmitted to the SLM equipment (Mlab Cusing 200R; Concept Laser GmbH). The frameworks were printed by direct laser metal sintering by using a powdered Co-Cr alloy (remanium Star CL, Powder 10-40 mm; Concept Laser GmbH) (60.5% Co, 28% Cr, 9% W, 1.5% Si, <1% Mn, <1% N, <1% Nb, <1% Fe, and elastic modulus of 230 GPa). The procedure specifications were based on the standard method recommended by the manufacturer: 25 μm of powder layer thickness and 200 W of Yb-fiber laser powder, with a maximum fabrication speed of 5 cm^3/h. Before the frameworks were removed from the building platform, they were heat treated in a furnace under argon atmosphere (1150 °C for 1 hour; cooling to 300 °C in the oven). This posttreatment is recommended by the manufacturer to eliminate the residual stresses of the printing procedure. Tungsten carbide burs at a low speed were used to remove the support structures, and the frameworks were finished with airborne-particle abrasion (125-μm Al_2O_3 particles; 0.55 MPa) according to the manufacturer's recommendation (Fig. 2C).

After all the frameworks had been manufactured, photoelastic stress analysis was performed. For the photoelastic model (PH model) fabrication, impression transfer copings for miniabutments were positioned on the master model. The transfers were united by using low-shrinkage autopolymerizing resin (GC Pattern Resin; GC America Inc) and a drill. The assembly was centrally positioned in a circular PVC section (4.5-cm diameter and 3.5-cm height) fixed on a glass plate by using utility wax (7 dental wax; Lysanda Produtos Odontologicos Ltd). The silicone (Silicone Master; Talmax Produtos de Protese Dentaria Ltd) was mixed according to the manufacturer's instructions and poured into the polyvinyl chloride (PVC) tube. After 48 hours, the impression transfer copings were loosened, and the master model was removed from the silicone

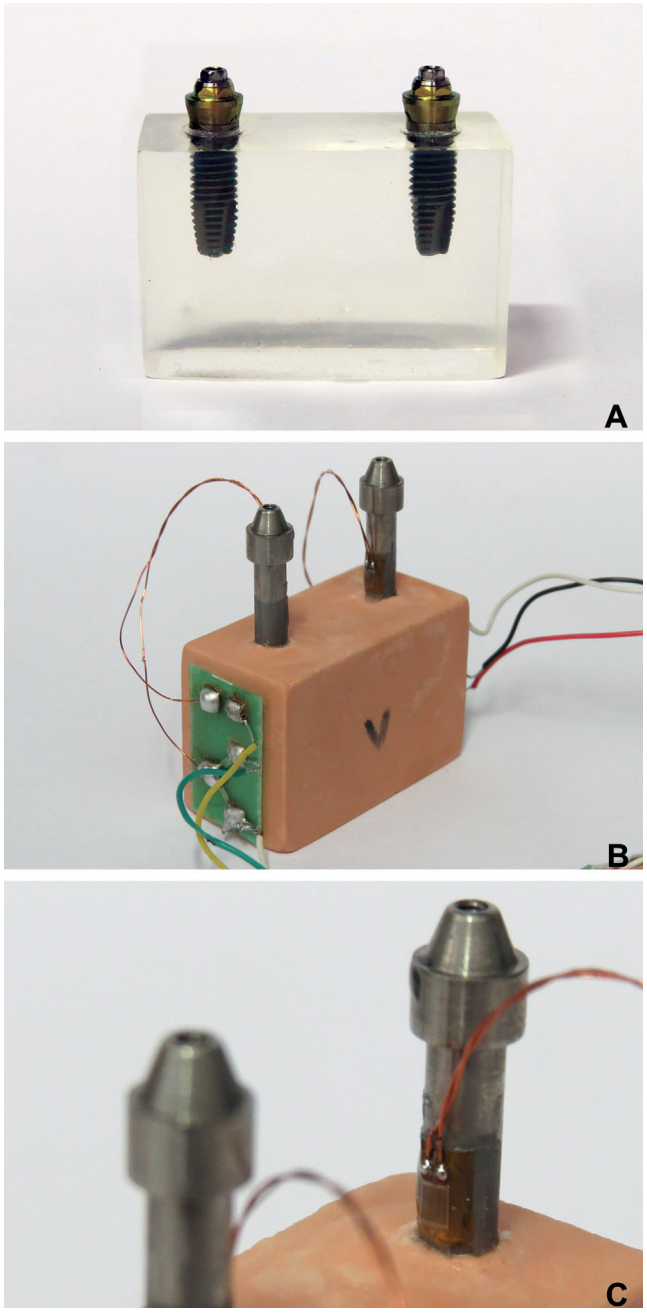

Figure 3. A, Photoelastic model. B, Strain gauge model with electric circuit in one-quarter of Wheatstone bridge. C, Positioning of strain gauges with strain axis perpendicular to base of model.

impression. The photoelastic resin (Araldite GY 279 BR and catalyst Aradur HY 2963; Araltec Chemicals Ltd) was manipulated for 1 minute at a resin-to-catalyst proportion of 2:1. The mixture was placed in a pressure chamber coupled to an air injection tube (5.9 MPa; 20 minutes) for bubble removal. Brånemark standard implants (Tryon external hexagon implant 4.1×11 mm; SIN-Sistema de Implante) with miniabutments (Miniabutment-external hexagon 4.1×2 mm; SIN-Sistema de

Implante) were tightened on the silicone matrix transfers. The photoelastic resin was slowly poured over the silicone matrix. After 72 hours, the transfers were removed, the PH model was obtained, and the translucency and surface finish were verified, making it appropriate for analysis (Fig. 3A).

Photoelastic analysis was performed by using a circular polariscope of horizontal transmission (developed in the Mechanical Design Lab Henner Alberto Gomide, School of Mechanical Engineering of the Federal University of Uberlandia), consisting of two 1/4-retardant wave filters and 2 polarizing filters, the polarizer and the analyzer. Markings on the polariscope platform were made to standardize the position of the model during analysis. The frameworks were tightened to the photoelastic model with a 10-Ncm torque and the tightening sequence PM-M. A layer of mineral oil was applied to the photoelastic model to improve the viewing of fringes. All measurements were performed on the same model. The images were acquired by using a digital camera (Canon SX50HS; Canon Inc), and the stress values were quantified by using a specific software program (Fringes software; Mechanical Design Lab, FMEC, Federal University of Uberlandia). For this purpose, 10 points of interest were determined along the entire length of each implant (Fig. 4). The formula s=KN/2b—where K=11.271 N/mm was the optical constant of the photoelastic resin, N was the fringe order, and b=15 mm was the thickness of the model—was used to calculate the maximum shear stress (τ) for each point, yielding the stress average for each region (PM and M) and the framework ($\frac{\text{PM region+M region}}{2}$).

Strain gauge analysis was performed to investigate the strain induced on the miniabutments. For fabrication of the strain gauge model (SG model), a similar transfer set of photoelastic models was fabricated on the master model. Modified conical dental implant abutment analogs were tightened on transfers. A parallelometer was used to place the transfer and analog assemblies perpendicular to the base in a silicone matrix with the same dimensions as the master model. The silicone matrix was filled with Type IV dental stone cast (Durone IV; Dentsply Sirona) manipulated according to the manufacturer's recommendations (19 mL of water and 100 g of powder for 30 seconds in a vacuum), and 9-mm long analog stems were embedded in the dental stone cast. Before model fabrication, the analog stems were abraded with 110-μm aluminum oxide particles at 0.55 MPa pressure to create a rough surface able to sustain strain gauge bonding. Two strain gauges (PA-06-060-BG-350 L; Excel Sensores Ltd) were bonded parallel to the long axis of the analogs by using cyanoacrylate-based adhesive (Loctite Super Bonder; Henkel). The electric circuit was mounted in a one-quarter Wheatstone bridge with temperature control (Fig. 3B, C). The SG model was connected to the ADS 2000 (Lynx Tecnologia Eletronica Ltd), with data processed by using a specific software program (AqAnalysis 2000; Lynx Tecnologia Eletronica Ltd). The tightening of frameworks on the model followed the same protocol as described for the photoelastic analysis. The frameworks were tightened on the model, and the average strain value was obtained with

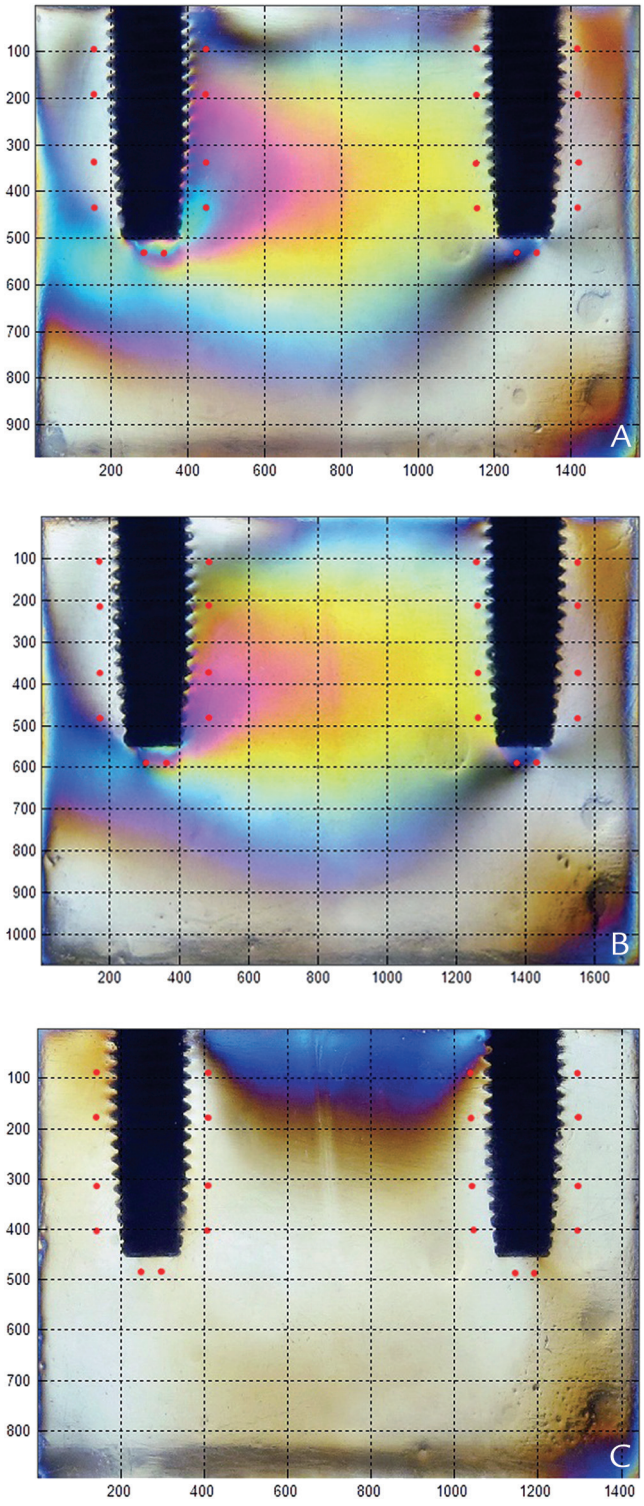

Figure 4. Ten points (*red*) of interest determined around each implant. A, Cast framework. B, SMB framework. C, SLM framework. SLM, selective laser melting; SMB, soft metal block.

a 5-minute interval, beginning 3 minutes after tightening. All measurements were performed on the same model. Between analyses, the strain gauges were set to zero to verify that there was no plastic deformation of the modified analogs.[5]

After the stress and strain analyses, the marginal fit (Fig. 5) was measured with the PH and SG models by using a 1.0-μm precision microscope at ×120 magnification (VMM-100-BT; Walter Uhl), equipped with a digital camera (KC-512NT; Kodo BR Electronics Ltd) and an analyzer unit (QC 220-HH Quadra-Check 200; Metronics Inc). The measurements were performed according to the single-screw test protocol[3,5] by a blinded, calibrated examiner (A.G.C.P.), where an intraclass correlation coefficient of 0.991 ($P<.001$) was obtained. The frameworks were placed in the models, the prosthetic screw of the PM region was tightened to 10 Ncm by using a 0.1-Ncm precision digital torque meter (Torque Meter TQ-8800; Lutron), and 2 readings of the discrepancy were obtained for the M region in the buccal and lingual regions of the abutment, diametrically opposed, at the abutment-prosthesis interface. The readings were standardized on the central portion of the miniabutment platform between the top edge and the prosthetic framework. The procedure was repeated with the M region, yielding an average fit value for each region (PM and M) and for each framework, $(\frac{\text{PM region+M region}}{2})$.

The Student *t* test was performed to evaluate the reproducibility of the transfer technique by comparing fit values of the master model and the working models (PH model and SG model). Data were subjected to the Kruskal-Wallis test to investigate the influence of the framework manufacturing method on the fit, stress, and strain values. The Mann-Whitney U test was used to compare the groups in pairs. The Spearman correlation test was used to evaluate the correlation between fit and stress or strain data. Analyses were conducted by using a specific software program (IBM SPSS Statistics, v21.0; IBM Corp) ($\alpha=.05$). The effect size of each test was determined statistically according to the Mann-Whitney U test ($r>0.846$).

RESULTS

No significant differences were found in the marginal fit between the models (master model-PH model: $t=-0.556$; $df=58$; $P=.580$; master model-SG model: $t=-0.312$; $df=58$; $P=.756$; PH model-SG model: $t=-0.261$; $df=58$; $P=.795$; Student *t* test). The framework manufacturing method affected the fit values ($P<.001$; Kruskal-Wallis test). The SLM group showed the best levels of mean ±standard deviation marginal fit (μm) (PH model, 8.4 ±3.2; SG model, 6.9 ±2.1) ($P<.05$), and no difference was observed between the SMB milled (PH model, 42.3 ±15.7; SG model, 41.3 ±15.3) and casting groups (PH model, 43.5 ±27.8; SG model, 41.3 ±24.6) ($P>.05$) (Fig. 6).

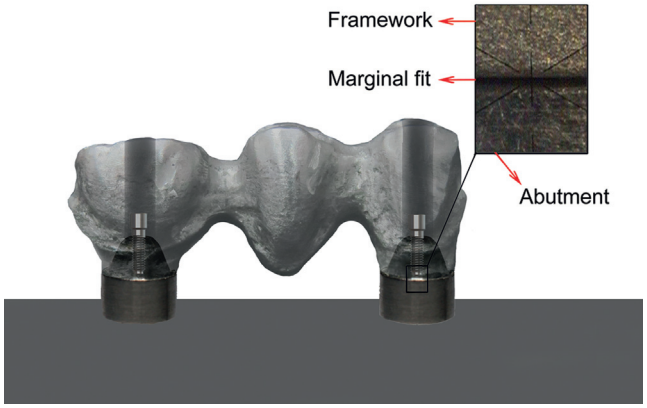

Figure 5. Schematic of marginal fit reading.

A significant influence of the framework manufacturing method on the stress and strain values was noted ($P=.001$, Kruskal-Wallis test). The SLM group showed the lowest mean ±standard deviation stress and strain levels (PH model, 60.3 ±11.6 MPa; SG model, 91.4 ±11.1 μstrain) ($P<.05$) (Fig. 6). No difference in mean ±standard deviation stress values was found between the SMB milled (PH model, 218.6 ±101.7 MPa; SG model, 289.7 ±89.3 μstrain) and casting groups (PH model, 225.5 ±142.8 MPa; SG model, 227.0 ±55.4 μstrain) ($P>.05$) (Fig. 7). Positive correlations between stress or strain and marginal fit were observed for all interactions (Table 1).

DISCUSSION

The findings of this study revealed that the dimensional precision of FPD frameworks depends on the manufacturing method. Thus, the first null hypothesis—no difference would be found in the dimensional precision of FPD frameworks manufactured by using the 3 different technologies—was rejected. FPDs frameworks made by SLM technology showed lower levels of marginal fit, stress, and strain. Also, the variations of marginal fit, stress, and strain values in the SLM group were lower, suggesting a higher reliability of the technology, than in the casting and SMB milled groups.

One possible reason for the improved dimensional precision and reliability of frameworks fabricated by the SLM technology is the achievement of 100% of the material's density at the final printing procedure.[21] In this study, posttreatment heat was applied to reduce the stresses in the SLM frameworks (1150 °C for 1 hour), and the full density of the material was achieved before this step. However, the full density of SMB frameworks was achieved only after the sintering step (1280 °C for 5 hours), which can induce shrinkage of up to 11%.[3] The shrinkage modifies the dimensional configuration of each framework differently, generating a within-group difference at the final procedure, and could explain the higher data distribution in the SMB group. The sintering step of

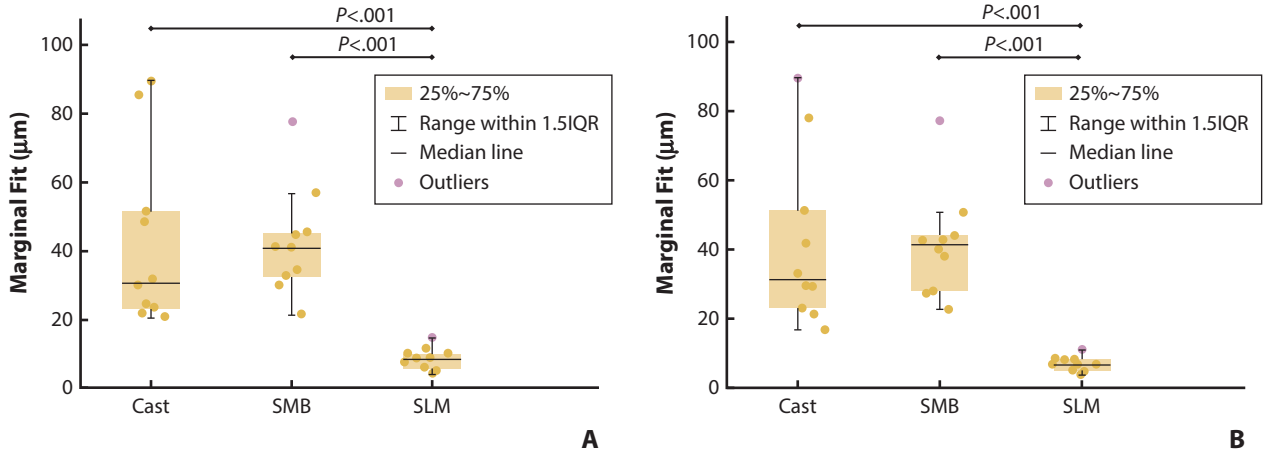

Figure 6. Box and scatter plots of marginal fit values (µm) of cast, SMB, and SLM frameworks. A, Photoelastic model. B, Strain gauge model. Groups connected by lines indicate differences between them ($P<.05$, Mann-Whitney U test). IQR, interquartile range; SLM, selective laser melting; SMB, soft metal block.

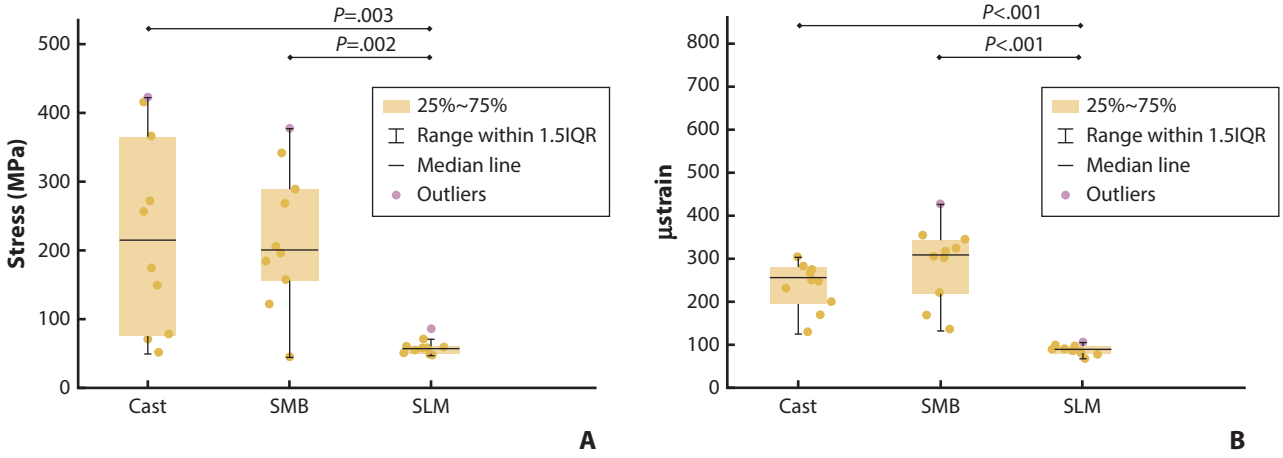

Figure 7. Box and scatter plots of stress values (MPa) of cast, SMB, and SLM frameworks. A, Photoelastic analysis. B, Strain gauge analysis. Stress and strain values represent stress or strain mean $\left(\frac{\text{PM region+M region}}{2}\right)$ of frameworks. Groups connected by lines indicate differences between them ($P<.05$, Mann-Whitney U test). IQR, interquartile range; M, first molar; PM, first premolar; SLM, selective laser melting; SMB, soft metal block.

the SMB has previously been reported as a reason for the fit similarity of the SMB technique with that of casting 3-unit FPDs.[3,5] Also, the similarity between the techniques can be explained by the presence of a premachined base of the cast cylinders that improves the framework fit. This feature makes the casting technique the gold standard. For this reason, the cast group was used as a control group in the present study.

Another reason in support of the superior dimensional precision of SLM frameworks is the different elastic modulus of alloy materials among the groups. Despite the fact that all frameworks were made with Co-Cr alloy, to isolate the influence of manufacturing methods, the alloy used for each system had specific compositions and properties, such as different elastic modulus values. Materials with higher elastic moduli are more resistant to deformation, resulting in lower stress transmission to the system.[13] Thus, the higher elastic modulus of the SLM alloy can explain the lower stress and strain data found in photoelastic and strain gauge analyses.

Both stress analyses allowed for the investigation of stress and strain parameters in the implant-supported system, except in the framework. The analysis could be performed by bonding the strain gauges on the frameworks, but it could introduce bias into the results because of the differences in positioning among the frameworks. Also, the bulk of the frameworks could lead to an inadequate measurement of strain.[5] Finite element analysis could provide stress data located inside the frameworks; however, the actual frameworks, in terms of porosity and density, cannot be accurately reproduced with this methodology. Despite the absence of information about stresses located in the frameworks, the indirect investigation of other components of implant-supported systems may suggest framework behavior.

In addition to the full-density achievement of SLM frameworks and their higher elastic modulus, the lower

Table 1. Spearmann correlation analysis between marginal fit and stress or strain as function of framework manufacturing method for both photoelastic and strain gauge models

	Marginal Fit/Stress-Strain Correlation			
Framework Manufacturing Method	**r**	***P*[a]**	**r[b]**	***P*[a,b]**
Casting				
Photoelastic model	0.915	<.001	0.883	.002
Strain gauge model	0.891	.001	0.867	.002
SMB				
Photoelastic model	0.903	<.001	0.883	.002
Strain gauge model	0.806	.005	0.733	.025
SLM				
Photoelastic model	0.930	<.001	0.904	.001
Strain gauge model	0.902	<.001	0.865	.003

[a]Significant $P<.05$ level (2-tailed). [b]Correlation values excluding outliers depicted in Figures 6 and 7 as red dots.

stress and strain values are also directly affected by their improved marginal fit because a positive correlation between stress or strain and marginal fit was observed, corroborating previous findings.[3] Studies comparing conventional casting and SLM technology also showed better marginal fit levels for the SLM technology for metallic copings[16,20] and FPDs.[10,12,17] Also, the present results are consistent with a previous fit investigation of implant-supported FPDs that reported better accuracy of the SLM technique than milling or conventional casting using Co-Cr alloy for 3-unit and 4-unit designs.[29] A more complete investigation of the marginal and internal fit of cemented Co-Cr 3-unit FPD frameworks made by SLM, conventional casting, and milling showed that the SLM technique was better than the milling method, corroborating the present findings.[19]

The superiority of the SLM technique in this study is also justified by the fact that there is no need for drilling compensation during the CAD file processing, which is needed for the SMB milled group.[19] This is because the smallest milling burs used had a 1.0-mm diameter, so the scanner software created a space on the internal straight angles to obtain access for them. The effect of this compensation was even more pronounced for cemented prostheses, leading to higher cement film thickness.[19] For implant-supported frameworks, evidence suggests that a more intimate prosthesis cylinder-to-abutment contact implies the higher stability of the implant-supported system.[5] Thus, a promising long-term behavior of SLM frameworks under the influence of dynamic loading may be predicted because there is no need for drill compensation with this technology; however, future investigations of internal fit and its correlation with marginal fit, stress, and strain variables after longer periods of simulated clinical use are required.

In the field of prosthodontics, new technologies are based on the premise of achieving higher quality prostheses. For 3-unit FPD frameworks, initial fit, stress, and strain results indicate that 3D printing SLM technology is a promising clinical option with reliability, improved fit levels, and, consequently, lower stress and strain transmitted to the implant-support system. However, the long-term performance of SLM frameworks cannot be determined, and research simulating longer clinical use is needed to clarify the influence of dynamic loading on the analyzed variables. Also, future research comparing other CAD-CAM systems and materials is necessary. Furthermore, longitudinal follow-up of implant-supported prosthetic rehabilitations with 3-unit FPDs fabricated by the evaluated manufacturing methods could support the long-term safety and efficacy of using the SLM technology in clinical practice.

CONCLUSIONS

Based on the findings of this in vitro study, the following conclusions were drawn:

1. The dimensional precision of 3-unit FPD frameworks is affected by the manufacturing method.
2. Three-unit FPD frameworks made by the SLM technology showed superior dimensional precision.

REFERENCES

1. Kim DY, Kim JH, Kim HY, Kim WC. Comparison and evaluation of marginal and internal gaps in cobalt-chromium alloy copings fabricated using subtractive and additive manufacturing. J Prosthodont Res 2018;62:56-64.
2. Jemt T, Henry P, Lindén B, Naert I, Weber H, Wendelhag I. Implant-supported laser-welded titanium and conventional cast frameworks in the partially edentulous law: a 5-year prospective multicenter study. Int J Prosthodont 2003;16:415-21.
3. Presotto AGC, Bhering CLB, Mesquita MF, Barão VAR. Marginal fit and photoelastic stress analysis of CAD-CAM and overcast 3-unit implant-supported frameworks. J Prosthet Dent 2017;117:373-9.
4. Abduo J, Lyons K, Bennani V. Fit of screw-retained fixed implant frameworks fabricated. Int J Prosthodont 2011;24:207-20.
5. Bhering CLB, Marques IDSV, Takahashi JMFK, Barão VAR, Consani RLX, Mesquita MF. The effect of casting and masticatory simulation on strain and misfit of implant-supported metal frameworks. Mater Sci Eng C Mater Biol Appl 2016;62:746-51.
6. Kim KB, Kim JH, Kim WC, Kim JH. Three-dimensional evaluation of gaps associated with fixed dental prostheses fabricated with new technologies. J Prosthet Dent 2014;112:1432-6.
7. Karl M, Holst S. Strain development of screw-retained implant-supported fixed restorations: procera implant bridge versus conventionally cast restorations. Int J Prosthodont 2012;25:166-9.
8. Romero GG, Engelmeier R, Powers JM, Canterbury AA. Accuracy of three corrective techniques for implant bar fabrication. J Prosthet Dent 2000;84:602-7.
9. de França DGB, Morais MHST, das Neves FD, Barbosa GA. Influence of CAD/CAM on the fit accuracy of implant-supported zirconia and cobalt-chromium fixed dental prostheses. J Prosthet Dent 2015;113:22-8.
10. Kim KB, Kim WC, Kim HY, Kim JH. An evaluation of marginal fit of three-unit fixed dental prostheses fabricated by direct metal laser sintering system. Dent Mater 2013;29:91-6.
11. Strub JR, Rekow ED, Witkowski S. Computer-aided design and fabrication of dental restorations: current systems and future possibilities. J Am Dent Assoc 2006;137:1289-96.
12. Pompa G, Di Carlo S, De Angelis F, Cristalli MP, Annibali S. Comparison of conventional methods and laser-assisted rapid prototyping for manufacturing fixed dental prostheses: an in vitro study. Biomed Res Int 2015;2015:3180-97.
13. Bhering CLB, Mesquita MF, Kemmoku DT, Noritomi PY, Consani RLX, Barão VAR. Comparison between all-on-four and all-on-six treatment concepts and framework material on stress distribution in atrophic maxilla: A prototyping guided 3D-FEA study. Mater Sci Eng C Mater Biol Appl 2016;69:715-25.

14. Kapos T, Ashy LM, Gallucci GO, Weber H-P, Wismeijer D. Computer-aided design and computer-assisted manufacturing in prosthetic implant dentistry. Int J Oral Maxillofac Implants 2009;24 Suppl:110-7.
15. Hjalmarsson L, Örtorp A, Smedberg JI, Jemt T. Precision of fit to implants: a comparison of cresco and procera implant bridge frameworks. Clin Implant Dent Relat Res 2010;12:271-80.
16. Sundar MK, Chikmagalur SB, Pasha F. Marginal fit and microleakage of cast and metal laser sintered copings-An in vitro study. J Prosthodont Res 2014;58:252-8.
17. Castillo-Oyagüe R, Lynch CD, Turrión AS, López-Lozano JF, Torres-Lagares D, Suárez-García MJ. Misfit and microleakage of implant-supported crown copings obtained by laser sintering and casting techniques, luted with glass-ionomer, resin cements and acrylic/urethane-based agents. J Dent 2013;41:90-6.
18. Ren X, Zeng L, Wei Z, Xin X, Wei B. Effects of multiple firings on metal-ceramic bond strength of Co-Cr alloy fabricated by selective laser melting. J Prosthet Dent 2016;115:1-6.
19. Örtorp A, Jönsson D, Mouhsen A, Vult Von Steyern P. The fit of cobalt-chromium three-unit fixed dental prostheses fabricated with four different techniques: A comparative in vitro study. Dent Mater 2011;27:356-63.
20. Xu D, Xiang N, Wei B. The marginal fit of selective laser melting-fabricated metal crowns: An in vitro study. J Prosthet Dent 2014;112:1437-40.
21. Van Noort R. The future of dental devices is digital. Dent Mater 2012;28:3-12.
22. Alharbi N, Wismeijer D, Osman R. Additive manufacturing techniques in prosthodontics: where do We currently stand? A Critical Review. Int J Prosthodont 2017;30:474-84.
23. Oyagüe RC, Sánchez-Turrión A, López-Lozano JF, Suárez-García MJ. Vertical discrepancy and microleakage of laser-sintered and vacuum-cast implant-supported structures luted with different cement types. J Dent 2012;40:123-30.
24. Kim EH, Lee DH, Kwon SM, Kwon TY. A microcomputed tomography evaluation of the marginal fit of cobalt-chromium alloy copings fabricated by new manufacturing techniques and alloy systems. J Prosthet Dent 2017;117:393-9.
25. Zhou Y, Li Y, Ma X, Huang Y, Wang J. Alternative method to evaluate the adaptation of implant-supported multi-unit prosthetic frameworks. J Prosthodont 2019;28:e643-8.
26. Krug K-P, Knauber AW, Nothdurft FP. Fracture behavior of metal-ceramic fixed dental prostheses with frameworks from cast or a newly developed sintered cobalt-chromium alloy. Clin Oral Investig 2015;19:401-11.
27. Nesse H, Ulstein DM, Vaage MM, Øilo M. Internal and marginal fit of cobalt-chromium fixed dental prostheses fabricated with 3 different techniques. J Prosthet Dent 2015;114:686-92.
28. Svanborg P, Tech D, Eliasson A, Stenport V. Additively manufactured titanium and cobalt-chromium implant frameworks: fit and effect of ceramic veneering. Int J Oral Maxillofac Implants 2018;33:590-6.
29. Akçin ET, Güncü MB, Aktaş G, Aslan Y. Effect of manufacturing techniques on the marginal and internal fit of cobalt-chromium implant-supported multiunit frameworks. J Prosthet Dent 2018;120:715-20.

Corresponding author:
Dr Valentim Adelino Ricardo Barão
Department of Prosthodontics and Periodontology
University of Campinas (UNICAMP)
Piracicaba Dental School
Av Limeira, 901, Piracicaba
Sao Paulo 13414-903
BRAZIL
Email: vbarao@unicamp.br, ricardo.barao@hotmail.com

Acknowledgments
The authors thank Paulo Pacheco and Paulo Inforçatti of Techno-How Engenharia Industrial e Comercio Ltd for the assistance and supplying the selective laser melting computer-aided design and computer-aided manufacturing frameworks and also Pedro Yoshito Noritomi and Henrique Takashi Idogava for the support in the selective laser melting frameworks fabrication. The authors are also grateful to Professor Mauro A. A. Nobilo for providing the polariscope facility.

https://doi.org/10.1016/j.prosdent.2019.01.019

Noteworthy Abstracts of the Current Literature

Relationship between selective serotonin reuptake inhibitors and risk of dental implant failure

Carr AB, Gonzalez RLV, Jia L, Lohse CM

J Prosthodont 2019 Mar;28:252-7

Purpose. To identify associations between implant failure and selective serotonin reuptake inhibitor (SSRI) medication use in a cohort of consecutive patients receiving dental implants during a 20-year period.

Material and methods. A retrospective review was conducted of all patients who received at least 1 dental implant from January 1, 1995, through December 31, 2014, assessing their history of SSRI use, active SSRI use, and SSRI use during follow-up with implant failure. Cox proportional hazards regression models assessed associations between demographic characteristics and SSRI use with implant failure, and outcomes were summarized with hazard ratios (HRs) and 95% confidence intervals (CIs). Follow-up SSRI use was analyzed with time-dependent covariates.

Results. During the study period, 5456 patients received their first implant (median age, 53 years). The median duration of follow-up was 5.3 years (interquartile range, 2.3-10.2 years) for the 4927 patients who did not have implant failure. For the 529 patients who had implant failure, it occurred at a median of 0.5 years. After adjusting for age, sex, and era of implant, history of use of the SSRI sertraline was associated with an increased risk of implant failure among all patients (hazard ratio [HR], 1.60; 95% CI, 1.15-2.23; P=0.006) and among the subset of patients with a history of SSRI use (HR, 1.64; 95% CI, 1.07-2.52; P=0.02).

Conclusions. In the population reviewed, a history of sertraline use was associated with a 60% greater risk of implant failure; however, active SSRI use at the time of implant placement or during follow-up was not significantly associated with an increased risk of implant failure.

Reprinted with permission of The American College of Prosthodontists.